

Mechanics of collisional motion of granular materials. Part 3. Self-similar shock wave propagation

By A. GOLDSHTEIN, M. SHAPIRO† AND C. GUTFINGER

Faculty of Mechanical Engineering, Technion-Israel Institute of Technology, Haifa 32000, Israel

(Received 2 November 1994 and in revised form 29 December 1995)

Shock wave propagation arising from steady one-dimensional motion of a piston in a granular gas composed of inelastically colliding particles is treated theoretically. A self-similar long-time solution is obtained in the strong shock wave approximation for all values of the upstream gas volumetric concentration ν_0 . Closed form expressions for the long-time shock wave speed and the granular pressure on the piston are obtained. These quantities are shown to be independent of the particle collisional properties, provided their impacts are accompanied by kinetic energy losses. The shock wave speed of such non-conservative gases is shown to be less than that for molecular gases by a factor of about 2.

The effect of particle kinetic energy dissipation is to form a stagnant layer (solid block), on the surface of the moving piston, with density equal to the maximal packing density, ν_M . The thickness of this densely packed layer increases indefinitely with time. The layer is separated from the shock front by a fluidized region of agitated (chaotically moving) particles. The (long-time, constant) thickness of this layer, as well as the kinetic energy (granular temperature) distribution within it are calculated for various values of particle restitution and surface roughness coefficients. The asymptotic cases of dilute ($\nu_0 \ll 1$) and dense ($\nu_0 \sim \nu_M$) granular gases are treated analytically, using the corresponding expressions for the equilibrium radial distribution functions and the pertinent equations of state. The thickness of the fluidized region is shown to be independent of the piston velocity.

The calculated results are discussed in relation to the problem of vibrofluidized granular layers, wherein shock and expansion waves were registered. The average granular kinetic energy in the fluidized region behind the shock front calculated here compared favourably with that measured and calculated (Goldshtein *et al.* 1995) for vibrofluidized layers of spherical granules.

1. Introduction

Vibrofluidized granular materials are widely used in various industrial processes. A common feature of many granular flows is their occurrence in the collisional regime. This means that the granules interact with each other through collisions which are responsible for momentum transfer and kinetic energy dissipation in the flow. These collisional flow regimes of non-conservative granular materials may be modelled on the basis of the kinetic theory of non-uniform gases (Chapman & Cowling 1970).

The kinetic theory is aimed at deriving the appropriate hydrodynamic equations governing granular flows (see Campbell 1990). These equations may be obtained on the

† To whom all correspondence should be addressed.

basis of an appropriately modified Boltzmann equation either by approximate methods of gas kinetic theory (Lun *et al.* 1984; Jenkins & Richman 1985*a, b*) or by a rigorous application of a variant of the Champan–Enskog solution scheme (Goldshtein & Shapiro 1995). The latter method has the advantage of yielding the right form of the hydrodynamic equations and, simultaneously, establishing their validity range. The latter is expressed in terms of the parameters of the collisional model chosen for calculations. In most cases these include the particle roughness β , and restitution coefficient (inelasticity) e (Lun 1991).

Such theories were developed for the rapid granular motion prevailing in shearing flows (e.g. see the review by Campbell 1990), and in fluidized beds (Homsy, Jackson & Grace 1992). Much less attention have been devoted to vibrofluidized rapid granular flows (see Savage 1988; Goldshtein *et al.* 1995). In this type of granular motion the collisional regime is sustained by virtue of work performed by the oscillating plate. This work is converted into kinetic energy of chaotic granular motion, which is then dissipated by means of particles' inelastic collisions. The physical mechanism responsible for conversion of work performed by the oscillating plate into kinetic energy of chaotic granular motions is not well understood.

This paper is a part of a long-term study, the ultimate aim of which is the development of a mathematical model of vibrofluidized granular layers. Specifically, we are interested in vibrofluidized granular motion occurring in the collisional regime. In our recent experimental work (Goldshtein *et al.* 1995) we observed compression (shock) and expansion waves propagating across vibrated granular layers composed of 5 mm glass beads. These processes appear to be responsible for the kinetic energy transfer between the averaged layer motion and granule random motion. Moreover, these waves were shown to govern the vibrational state of granular layers, which is characterized by granular energy (temperature), density and pressure. This study is thus devoted to theoretical investigations of the wave propagation process within granular layers. Specifically, we consider shock wave propagation within a system of solid particles. A comparable problem for the expansion wave, which is also relevant to modelling vibrofluidization of granular layers, is treated in a companion paper (Goldshtein, Shapiro & Gutfinger 1996).

The hydrodynamic equations used for modelling shear-induced flows are of the Navier–Stokes type, i.e. they are endowed with viscosity and conductivity terms (Campbell 1990). In one-dimensional *shearless* granular flows, like those prevailing in vibrated layers, these effects are insignificant since they are dominated by shock waves, which result from the granular gas compressibility. Accordingly, the hydrodynamic equations governing these wave propagation processes are of the Euler type. Such equations were derived by Goldshtein & Shapiro (1995) for rigid spherical particles of arbitrary (not necessarily small) inelasticity and roughness.

Wave propagation through an inviscid gas is one of the classical problems of compressible fluid dynamics (Courant & Friedrichs 1948). Unlike in molecular gases the motion of a granular medium is characterized by losses of granular kinetic energy induced by particle non-conservative collisions. The motion of a gas of such particles is described by appropriate hydrodynamic equations, explicitly accounting for the collisional losses. The objective of this work is to use these equations in order to describe the propagation of a stationary shock wave. This is done on the basis of the model problem of a piston moving with a constant speed into a granular gas of a uniform density filling the semi-infinite domain.

The existence of such a shock wave in a dissipative granular gas may be illustrated by the following simple considerations. Consider a solid piston moving with a finite

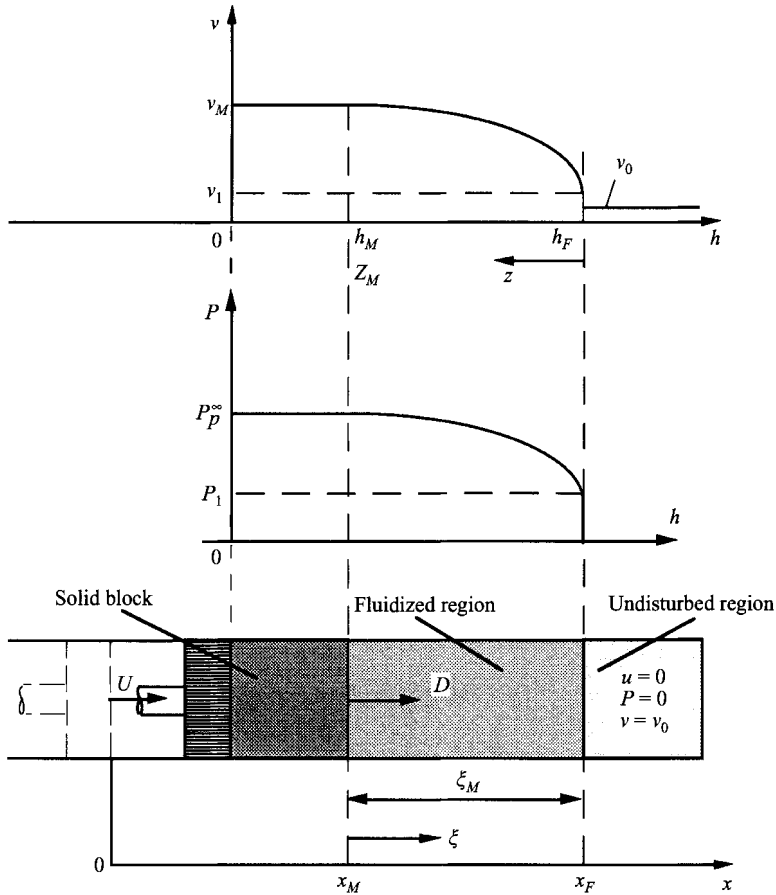


FIGURE 1. Schematic of the shock wave problem.

speed U into a cold motionless gas of a zero granular temperature in the absence of gravity. Supposing that the gas hydrodynamic properties change continuously, the disturbed domain propagates with the speed of sound, a , of the granular gas. Far from the piston this gas will inevitably have a zero temperature (kinetic energy) as a result of collisional energy losses. Therefore, the disturbances induced by the piston will propagate with the speed a , which is close to zero. On the other hand, since the disturbed domain cannot *decrease*, this speed cannot be less than U . Hence, no continuous (i.e. shockless) granular flow can exist. Rather, one can expect that a shock front is formed propagating into the granular gas with a velocity D exceeding the piston speed U .

In this paper we investigate the effect of granular properties on the shock wave speed D and the gas hydrodynamic properties in the disturbed domain between the shock front and the piston.

Granular gas gains kinetic energy when passing through the shock front. Inelastic non-conservative collisions lead to a continuous decrease of this granular energy and, hence, the pressure behind the front. As a result, a layer of densely packed granules (which have completely lost their kinetic energy) is formed on the moving piston. The formation of such a layer, which has a finite density which is the maximal possible that may be achieved within granular media, constitutes a specific feature distinguishing non-conservative systems from molecular gases. This phenomenon was disregarded by

Matveev (1983) who treated a related problem of sedimentation of a granular gas on a solid plate, where infinite gas density was obtained.

The densely packed layer is separated from the shock front by a fluidized region. Determination of the collisional state of the granular gas within this region, and the shock wave speed D , constitute specific goals of our treatment. These parameters, which are controlled by granular collisional properties, as obtained by the solution for the infinite layer, are then used to interpret the *ad hoc* solution (Goldshtein *et al.* 1995), developed for a periodically vibrated layer of *finite* thickness.

Other possible applications of the solution developed here include various technological processes involving powders and dusts in low-pressure conditions, and the interaction between a projectile and a loosely packed granular bed.

2. Governing equations

2.1. Euler hydrodynamic equation

Consider an ensemble of identical inelastic rough spherical particles – granules of diameter σ , mass m and density ρ_p – performing chaotic translational and rotational motions. The particles are assumed to be sufficiently heavy that the effect of the drag force (resulting from interactions with the surrounding gas) on their motion is negligible. We consider one-dimensional granular gas flow in a semi-infinite domain bounded by a piston moving in a tube of a constant (unit) cross-section along the x -axis (see figure 1).

It will prove convenient to describe the motion of the granular gas in Lagrangian coordinates (Courant & Friedrichs 1948) which are time variable, t , and the mass variable h :

$$h = \int_0^x \rho(\xi) d\xi.$$

Neglecting the effect of gravitational force, and thermal ‘conductivity’ and ‘viscosity’ of the granular gas, one obtains the equations for conservation of mass, momentum and energy in the Lagrangian representation (Goldshtein *et al.* 1995):

$$\frac{\partial}{\partial t} \left(\frac{1}{\rho} \right) = \frac{\partial u}{\partial h}, \quad \frac{\partial u}{\partial t} + \frac{\partial P}{\partial h} = 0, \quad \frac{\partial}{\partial t} \left(\frac{E}{m} \right) + P \frac{\partial u}{\partial h} = I, \quad (1a-c)$$

where $\rho = mn = \nu\rho_p$ is the bulk mass density, n is the particle number density, ν is the solids fraction (volume of solids per unit volume of the gas), u is the bulk hydrodynamic velocity, E is the total energy of particles’ random motion, P is the (hydrostatic) granular pressure, and I is the volumetric sink term, accounting for particle kinetic energy losses occurring during their collisions.

The density ρ of the granular medium may change from arbitrary small values up to a maximal value ρ_M , corresponding to the most densely packed state of incompressible solid granules. The mass and momentum conservation equations (1a, b) are valid for any continuum. Accordingly, they may be used for the granular medium prevailing both in fluidized and densely packed states, i.e. $0 < \rho \leq \rho_M$. In contrast, the kinetic energy equation will be considered only in the fluidized state, i.e. $0 < \rho < \rho_M$. The above equations require a constitutive relationship for the sink term, and an equation of the granular gas state. These equations relate P and I with other hydrodynamic and mechanical properties of the colliding granules. Additionally, modelling of flows of rough particles requires knowledge of the kinetic energy partition between the translational and rotational modes.

Equation of state	Range of ν	$g(\nu)$	Reference
$P = P_k = \frac{E}{2m} \alpha_t \nu \rho_p$	$\nu \ll 1$	1	Chapman & Cowling (1970)
$P = P_k[1 + 4\nu g_{CS}(\nu)]$	$0 \leq \nu < 0.5$	$g_{CS}(\nu) = \frac{2-\nu}{2(1-\nu)^3}$	Carnahan & Starling (1969)
$P = \left(\frac{\rho_M}{m}\right) T_t \left(\frac{3}{\Delta}\right)$	$1 - \nu/\nu_M \ll 1$	$g_M(\nu) = \frac{3}{4}(\Delta \nu_M)^{-1}$	Alder & Hoover (1968)
Equation (4)	$\nu \sim \nu_M$	$g_o(\nu) = [1 - (\nu/\nu_M)^{1/3}]^{-1}$	Ogawa <i>et al.</i> (1980)
Equation (4)	$0 \leq \nu < 0.55$	$g_{LS}(\nu) = (1 - \nu/\nu_M)^{-5\nu_M/2}$	Lun & Savage (1986)
Equation (4)	$0 \leq \nu < \nu_M$	$g(\nu) = [1 - (\nu/\nu_M)^{4\nu_M/3}]^{-1}$	Present

TABLE 1. Equilibrium radial distribution functions and corresponding equations of state

Constitutive relationships for the above equations have been obtained in several studies dealing with vibrofluidized motion (Raskin 1975) and rapid granular flows (Jenkins & Richman 1985*a, b*; Lun & Savage 1986, 1987; Lun *et al.* 1984; Lun 1991). These works employed different transport equations, adopted from kinetic theories of molecular gases (Grad 1949; Condiff, Lu & Dahler 1965; Chapman & Cowling 1970; McCoy, Sandler & Dahler 1966; Theodosopulu & Dahler 1974) together with several *ad hoc* hypotheses pertaining to the particle distribution function.

We use the constitutive relationship and the state equation, which were recently obtained (Goldshtein & Shapiro 1995) by rigorously solving the Boltzmann equation, which was appropriately modified to include a fairly general particle collisional model. This also provides the kinetic energy partition between rotational and translational modes and expressions for the sink term I , appearing in (1*c*). The average energy E of particle random motion may be expressed via granular kinetic translational T_t and rotational T_r temperatures in the following standard form:

$$T_t = \frac{1}{2}E\alpha_t, \quad T_r = \frac{1}{2}E\alpha_r, \quad T_t + T_r = \frac{2}{3}E, \quad (2a-c)$$

where translational $\frac{1}{2}\alpha_t$ and rotational $\frac{1}{2}\alpha_r$ constant-pressure specific heats depend upon mechanical collisional and inertial particle properties (see the Appendix).

The general equation of state of the granular gas can be written in the form (Goldshtein & Shapiro 1995)

$$P = P_k + P_c, \quad P_k = \frac{E}{2m} \alpha_t \nu \rho_p, \quad P_c = P_k[1 + 2(1+e)\nu g(\nu)], \quad (3a-c)$$

where P is the granular pressure, which is composed of collisional (P_k) and kinetic (P_c) parts and $g(\nu)$ is the equilibrium radial distribution function, which is independent of particle collisional properties and may be evaluated from the equation of state for a rigid elastic sphere gas model. Equations (3*a-c*) may be combined to yield the following equation of state:

$$P = \frac{E}{2m} \alpha_t \nu \rho_p [1 + 2(1+e)\nu g(\nu)]. \quad (4)$$

The above constitutive equation does not account for the granular gas viscosity, which is irrelevant in the present case of one-dimensional shearless motion (see also Goldshtein & Shapiro 1995; Goldshtein *et al.* 1995).

Several approximations suggested for $g(\nu)$ are summarized in table 1. In the simplest

case of a dilute granular gas (when the mean free path of the rigid-spheres system is much larger than their diameter) $g(\nu) = 1$ and the corresponding equation of state is equivalent to the ideal gas equation.

Alder & Hoover (1968) suggested an approximation for g , and the corresponding equation of state, which are valid when ν is close to the maximal packing density ν_M . Other correlations (Carnahan & Starling 1969; Ogawa, Umemura & Oshima 1980; Lun & Savage 1986) are valid up to intermediate values of ν , i.e. they reproduce the dilute gas expressions, but fail to comply with the high-density model of Alder & Hoover (1968).

In this work we use the following approximation for g :

$$g(\nu) = [1 - (\nu/\nu_M)^{4\nu_M/3}]^{-1}, \quad (5)$$

which is accurate for both of the above limiting situations.

The sink term for the collisional model (3a, b) has the following form (Goldshtein & Shapiro 1995):

$$I = C_0 \sigma^2 n g(\nu) \left(\frac{E}{m}\right)^{3/2} + \frac{\partial u}{\partial h} \frac{E}{2m} \alpha_t \nu \rho_p [C_1 + 2C_2(1+e)\nu g(\nu)], \quad (6)$$

where C_i ($i = 0, 1, 2$) are functions of particle inelasticity e , and roughness, β (see (A 4)–(A 11)), and were investigated in Part 1 (Goldshtein & Shapiro 1995). In particular, these coefficients vanish for conservative gases, i.e. $e = |\beta| = 1$.

Special consideration should be given to the case $\nu \rightarrow \nu_M$. In this singular limit the function $g(\nu)$ and the expression in square brackets on the right-hand side of (4) tend to infinity. This means that in such a limiting situation a granular gas may have a vanishingly small kinetic energy, but a finite pressure. This singular limit will be further discussed in §3, in relation to the pressure P prevailing in the solid block accumulating at the moving piston.

It should be noted that the energy equation is valid provided that the granular material behaves like a fluid, i.e. the random velocities of any two granules are not correlated. This means that no clusters are formed within the material. Such clusters have been shown to form in simple shear granular flows (Lun & Bent 1994). The formation of these structures in wavy motion can be investigated by computer simulations (Luding, Herrmann & Blumen 1994; Lan & Rosato 1995). However, the mass and momentum equations of type (1a, b) are applicable also to the case where clusters are present.

2.2. Conditions on the shock front

As in classical gas dynamics the problem of shock wave propagation requires formulation of the jump conditions for the hydrodynamic quantities across the discontinuity (the Rankine–Hugoniot condition). These conditions for non-conservative granular gases were obtained (Goldshtein & Shapiro 1995) in the Euler coordinate system. Noting that (1a, b) are explicitly independent of particle roughness and inelasticity, the jump conditions derived from the momentum and mass equations are the same as those for an ordinary gas (see Courant & Friedrichs 1948). Bearing in mind the relation between the kinematic speed, D , and the mass speed of the shock front, $D_L = (D - u)\rho$, one obtains the Rankine–Hugoniot conditions for the granular gas in the Lagrangian representation:

$$[u + D_L/\rho] = 0, \quad [P - D_L u] = 0, \quad (7a, b)$$

$$D_L \left[\frac{E}{m} + \frac{P}{\rho} + \frac{D_L^2}{2\rho^2} \right] = -\{C_1 P_k + C_2 P_c\} [u]. \quad (7c)$$

Here D_L is the Lagrangian shock wave velocity and for any hydrodynamic quantity ϕ (i.e. u, ρ, P), the symbols $[\dots], \{\dots\}$ denote $[\phi] = \phi_0 - \phi_1, \{\phi\} = (\phi_0 + \phi_1)/2$, with ϕ_0 and ϕ_1 being the respective values of ϕ before and after the discontinuity.

In §3 we employ a particular case of conditions (7), namely the strong shock wave approximation (Courant & Friedrichs 1948). In this case energy E_0 and pressure P_0 before the shock front are much smaller than their corresponding values E_1, P_1 behind the shock wave and the jump conditions (7) reduce to the following strong shock wave conditions:

$$u_1 = \frac{D_L}{\rho_0} - \frac{D_L}{\rho_1}, \quad P_1 = \frac{D_L^2}{\rho_0} - \frac{D_L^2}{\rho_1}, \quad (8a, b)$$

$$\frac{\rho_1}{\rho_0} - 1 = \frac{4}{\alpha_t(C_2 - C_1 + (1 - C_2)P/P_k)|_1} = \frac{4}{\alpha_t[1 - C_1 + (1 - C_2)2(1 + e)\nu_1 g(\nu_1)]}. \quad (8c)$$

Consider now these strong shock wave conditions in the limiting cases of dilute and dense gases. For a dilute gas model ($\nu \ll 1$) equations (8a, b) do not change while (8c) reduces to

$$\rho_1 = \rho_0 \left[1 + \frac{4}{\alpha_t(1 - C_1)} \right]. \quad (9)$$

Introducing the adiabatic exponent γ

$$\gamma = 1 + \frac{1}{2}\alpha_t(1 - C_1) \quad (10)$$

one can rewrite (9) in the familiar form of Rankine–Hugoniot conditions for molecular gases (see Courant & Friedrichs 1948):

$$\frac{\rho_1}{\rho_0} = \frac{\gamma + 1}{\gamma - 1}. \quad (11)$$

Therefore, for a dilute granular gas model, particle roughness and inelasticity affect shock wave conditions only via γ . This parameter attains the following values in the limiting (conservative) cases: (i) perfectly smooth elastic particles: $e = 1, \beta = -1, \alpha_t = 4/3, \gamma = 5/3$; (ii) perfectly rough elastic particles: $e = 1, \beta = 1, \alpha_t = 2/3, \gamma = 4/3$. For a non-conservative *dilute* granular gas the effect of the kinetic energy losses on this property is represented by the factor $(1 - C_1)$. This factor is the first-order contribution (proportional to the velocity gradient) to the sink term (6), changing the translational specific heat $\alpha_t/2$ by a factor of $(1 - C_1)$.

For the *dense gas model* (see table 1) jump conditions (8a–c) reduce respectively to

$$u_1 = \frac{A_0 D_L}{\rho_M} \left(1 - \frac{A_1}{A_0} \right), \quad P_1 = \frac{A_0 D_L^2}{\rho_M} \left(1 - \frac{A_1}{A_0} \right), \quad A_1 = A_0/\chi(e, \beta), \quad (12a-c)$$

where

$$\chi(e, \beta) = 1 + \frac{8}{3\alpha_t(1 - C_2)(1 + e)}. \quad (12d)$$

One can see that the first-order contribution to the sink term (6) increases the translational constant-pressure specific heat $\alpha_t/2$ of a *dense* granular gas by factor of $(1 - C_2)$.

The above simple conclusions about the influence of the sink term on the strong shock wave conditions are valid for the limiting case of dilute and high-density granular gas models only.

3. The shock wave problem

3.1. Problem formulation

Consider a semi-infinite ($x > 0$) tube uniformly filled with a ‘cold’ quiescent granular gas, bounded by a piston initially located at $x = 0$. The gas initial upstream (marked by subscript 0) hydrodynamic quantities are specified by the following initial conditions:

$$P_0 = 0, \quad E_0 = 0, \quad u_0 = 0, \quad \nu_0 = \text{const} \neq 0, \quad t < 0. \quad (13a)$$

Assume that beginning at time $t = 0$ the gas is set in motion by a piston propagating in the positive direction with a constant speed U . We describe the flow of the granular gas in a *stationary* frame with the origin $x = 0$ located at the initial position of the piston. This allows us to set the following boundary condition:

$$u = U \quad \text{at} \quad x = Ut \quad \text{or} \quad h = 0. \quad (13b)$$

In the circumstances described by the above initial and boundary conditions the moving piston generates a shock wave, the front of which propagates with a (time-dependent) speed D , or the corresponding mass speed $D_L = D\rho_0$. We denote by ν_1, u_1, P_1 the granular gas properties immediately behind the shock front. For classical (conservative) gases the distribution of these quantities between the piston and the shock front is uniform. This is no longer true for the granular gas, which is characterized by the particles’ collisional kinetic energy losses. Those particles which have completely lost their kinetic energy form a dense layer (solid block), of the maximal possible volumetric density ν_M , on the piston surface, the thickness of which, x_M (or h_M) grows with time (see figure 1). Particles in the region between the shock front and the densely packed layer prevail in an agitated or fluidized hydrodynamic state, which is governed by the Euler hydrodynamic equations (1)–(4), (6). These equations with the appropriate radial distribution function, given by (5), should be solved in the domain $x_M < x < x_F$, (or $h_M < h < h_F$) where x_F, h_F are the (time-dependent) kinematic and mass front locations. The corresponding jump conditions at the shock front, necessary for the solution, are given by (8a–c).

For conservative systems the sink term on the right-hand side of (1c) is zero. The problem of shock wave propagation through such a gas admits a similarity solution of the type

$$\psi = \psi(tD_L^0 - h), \quad t > 0, \quad (14)$$

where ψ is any of the hydrodynamic properties (velocity, density, pressure) and D_L^0 is a *constant* shock wave propagation speed (Courant & Friedrichs 1948). Moreover, the hydrodynamic properties ρ_1, u_1, P_1 in the region between the shock front and the piston are constants, which together with D_L^0 are determined from boundary conditions (13) and jump conditions (8a–c) upon setting $C_1 = C_2 = 0$.

In contrast to molecular gases, flowing non-conservative granular systems lose their random-motion kinetic energy E at a rate described by the sink term I in (6). This term introduces a certain timescale, t_s , which characterizes the rate of kinetic energy dissipation, and which does not allow similarity solutions of the type shown in (14). In particular, here the mass shock wave speed is a time-dependent function $D_L = D_L(t)$. In order to understand the process of wave propagation in non-conservative systems, suppose that the granular gas is characterized by small kinetic energy losses (i.e. e and $|\beta|$ are both close to 1). Clearly, for short times ($t \ll t_s$), when the kinetic energy losses are small, such a (‘almost conservative’) granular gas will behave like a conservative gas. In particular, for such short times one can expect that $D_L(t) \sim D_L^0$. However, with

increasing time, owing to kinetic energy losses the gas energy E_1 and, hence, the pressure P_1 immediately behind the front decrease, which inevitably leads to a concomitant decrease of D_L . On the other hand, the shock speed cannot be lower than, or even equal to, the speed of the piston U , since this contradicts the basic mass conservation law. Therefore, at least for large times one has

$$\rho_0 U < D_L(t) < D_L^0. \quad (15a)$$

On the other hand, the shock wave cannot disappear, in the sense that a continuous density distribution cannot exist everywhere. Otherwise, one encounters a situation where infinitesimal density disturbances propagate with the speed of sound a_0 in the undisturbed domain, where the granular temperature is zero, and hence $a_0 = 0$.

The above observation of a (large-time) temporal diminution of $D_L(t)$ leads to the conclusion that the shock front speed will eventually approach a certain limiting value D_L^∞ :

$$D_L(t) \rightarrow D_L^\infty \quad \text{when} \quad t \rightarrow \infty. \quad (15b)$$

Consequently, for times greatly exceeding the characteristic value t_s (which will be estimated in the discussion section) the speed $D_L(t)$, the hydrodynamic properties $\rho_1(t)$, $u_1(t)$, $P_1(t)$ immediately behind the shock front approach constant values. This steady wave propagation regime is determined by the balance between the power generated by the moving piston and the rate of granular energy losses in the fluidized region. One can, therefore, expect that these properties will approach their stationary forms:

$$u = u(z), \quad \rho = \rho(z), \quad P = P(z), \quad (16a-c)$$

where

$$z = \int_0^t D_L(t) dt - h = D_L^\infty t - h + h_0, \quad t \gg t_s \quad (16d)$$

is the coordinate relative to the shock front, with the constant h_0 being

$$h_0 = \int_0^\infty [D_L(t) - D_L^\infty] dt.$$

The solution (16a-c) is valid only in the fluidized region $0 \leq z \leq Z_M$, where Z_M is its thickness, which also reaches a constant asymptotic long-time value. However, (16d) implies that

$$Z_M = D_L^\infty t - h_M + h_0. \quad (17)$$

This means that the amount h_M of the material within the dense layer also increases with the rate D_L^∞ .

The large-time solution (15b)–(17) will be *a posteriori* verified by determination of the functions (16a-c) in such a way that they obey the governing equations and boundary and jump conditions.

This ultimate thickness Z_M of the fluidized region is to be determined from the solution of the problem. Therefore, an additional boundary condition at $z = Z_M$ should be specified. This is provided by noting that at the most dense state any random particle motion is impossible and the particle hydrodynamic velocity is equal to the piston speed, i.e.

$$v = v_M, \quad u = U, \quad E = 0, \quad P = P_p^\infty = \text{const} \quad \text{at} \quad z = Z_M, \quad (18a-d)$$

where P_p^∞ is the constant pressure prevailing in the densely packed domain $z \geq Z_M$, the value of which will be determined below. Since the density in (18a) reaches its maximal value and the kinetic energy vanishes, the point $z = Z_M$ is singular and condition (18d)

ensures that the pressure in this point is neither zero nor infinite. Mathematically conditions (18) constitute the requirement of continuity imposed on all hydrodynamic quantities in the region between the shock front and the piston. The physical significance of a non-zero pressure within the solid block is that the piston performs work at the rate $P_p^\infty U$, which is used to compensate the granular kinetic energy losses in the fluidized region due to particle collisions.

The problem of shock wave propagation through a granular gas, as formulated above for a quiescent gas before the front, represents the strong shock wave problem. We note that the assumption $E_0 = P_0 = 0$ used in (13a) places no physical limitation on the stationary solution (16a-c). Indeed, the latter is valid only for long times, at which the kinetic energy in the undisturbed region has decayed to zero, even if initially the granular gas had $E_0 \neq 0$.

Introduce solution (16a-d) into (1a, b) and integrate them subject to (8a, b), to express the bulk velocity u and the granular pressure P via the bulk density ρ :

$$u(\rho) = D_L^\infty \left(\frac{1}{\rho_0} - \frac{1}{\rho(z)} \right), \quad P(\rho) = (D_L^\infty)^2 \left(\frac{1}{\rho_0} - \frac{1}{\rho(z)} \right). \quad (19a, b)$$

Conditions (18a, b) together with (19a, b) yield the following expressions for the shock wave speed and pressure at the edge of the dense layer for the stationary shock wave motion:

$$D_L^\infty = \frac{U\rho_0}{1 - \rho_0/\rho_M}, \quad P_p^\infty = UD_L^\infty. \quad (20a, b)$$

Substituting the trial solution (16a-d) into (1c) with the sink term given by (6), one obtains the following ordinary differential equation:

$$D_L^\infty \frac{d}{dz} \left(\frac{E}{m} \right) + \frac{Ev\rho_p \alpha_t}{2m} [(1 - C_1) + 2(1 - C_2)(1 + e)vg(v)] \frac{d}{dz} \left(\frac{D_L^\infty}{\rho} \right) = \frac{\sigma^2 C_0}{m} \rho g(v) \left(\frac{E}{m} \right)^{3/2}. \quad (21)$$

Equation (19b) in combination with equation of state (4) enable us to rewrite the differential equation (21) in terms of the function $\rho = \rho(z)$. This equation does not include the piston speed U , since every term is proportional to U^3 . In addition v_M in the boundary conditions (18a) is also independent of U and so is the density ν_1 appearing in the jump condition (8c) at the shock front by virtue of the strong shock wave approximation. Bearing in mind the above, and simple dimensional considerations, one can write (17) in the form (cf. (39))

$$Z_M = \sigma\rho_M k_z(e, \beta, \nu_0, \nu_M),$$

which is independent of U .

Equation (21) is investigated in §§3.2 and 3.3 for different approximations of the radial distribution function considered in §2.1. A particular case of this problem, pertaining to a highly dense granular gas, enables one to obtain a closed form analytical solution, outlined in §3.2.

We analyse expressions (20a, b) for the shock wave speed and pressure at the edge of the dense layer. One can see that these quantities are independent of the particle collisional properties and specific heats. This is in contrast with the comparable results for molecular gases (Courant & Friedrichs 1948), namely

$$D_L^0 = \frac{\rho_0 U}{1 - \rho_0/\rho_1}, \quad P_L^0 = UD_L^0, \quad (22a, b)$$

where ρ_1 is related to ρ_0 via expression (8c).

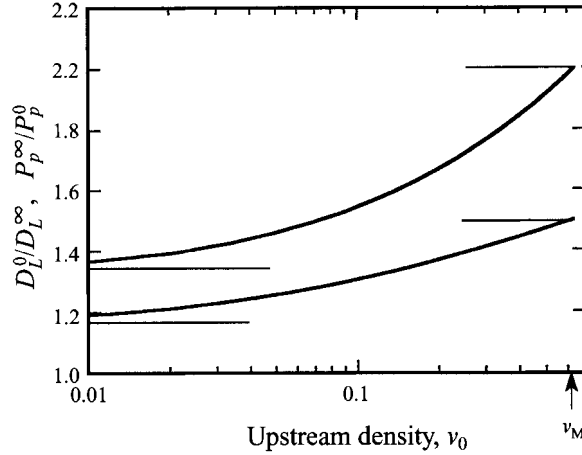


FIGURE 2. Ratios of the shock wave speeds and pressures behind the front of conservative (molecular, D_L^0, P_L^0) and non-conservative (granular, D_L^∞, P_L^∞) gases. Data for molecular gases are calculated for $e = 1$, and $\beta = -1$ (upper lines) and $\beta = 1$ (lower lines). Straight lines: dilute and dense gas limits.

The ratios of the classical and granular gas ultimate shock wave speeds and pressures behind the shock wave are shown in figure 2. D_L^0 is seen to be larger than its non-conservative analogue D_L^∞ , and this is clearly explained by the kinetic energy losses, which increase with increasing ν_0 causing, thereby, the concomitant increase of D_L^0/D_L^∞ . This ratio reaches a maximum in the limiting case of the highest initial density and a minimum for the dilute upstream gas. In all the cases the effect of non-conservative collisions results in no more than a 50% diminution of D_L^∞ relative to D_L^0 . Smooth particles lose their kinetic energy faster (per collision), since their rotational degrees of freedom are excluded from the energy partition. Therefore for these particles the ratio D_L^0/D_L^∞ is larger than for rough particles.

Limiting values of D_L^∞ for $\nu_0 \rightarrow 0, \nu_M$ may be calculated analytically. In particular, in the case of a dilute gas one can use (11) to obtain

$$D_L^0/D_L^\infty = (\gamma + 1)/2, \quad \nu_0 \rightarrow 0.$$

For perfectly elastic ($e = 1$) smooth ($\beta = -1$) spheres, $\gamma = 5/3$ which yields $D_L^0/D_L^\infty = 4/3$. For perfectly elastic rough particles ($\beta = 1$), one gets $D_L^0/D_L^\infty = 7/6$.

The shock speed ratio in the dense limit may be evaluated using (12c, d):

$$D_L^0/D_L^\infty = 1 + 3\alpha_t/4, \quad \nu_0 \rightarrow \nu_M.$$

For perfectly elastic smooth spheres $\alpha_t = 4/3$ and the above limiting value is equal to 2. In the comparable case of perfectly elastic rough particles $\alpha_t = 2/3$, which yields $D_L^0/D_L^\infty = 3/2$.

The fundamental difference between the shock speeds of conservative and granular gases emphasizes the singular character of the limits $e \rightarrow 1, |\beta| \rightarrow 1$, where the kinetic energy losses in the granular gas approach zero. Expressions (20a, b), which are valid even for infinitesimally small losses, differ markedly from the corresponding expressions (22) for conservative gases. This means that even for very small inelasticities the state of the granular gas will ultimately approach the solution (16a-d), with the corresponding e - and β -independent shock wave speed (20a). These collisional parameters will, however, affect the *rate of approach* of the exact solution to its ultimate asymptotic self-similar form. Clearly, as the kinetic energy losses tend to zero, the

characteristic time of this approach tends to infinity, as does the constant value h_0 , characterizing the (mass) distance covered by the shock wave until it reaches its ultimate speed. This distance cannot be determined from the asymptotic solution; its calculation requires obtaining a more general solution which is valid for shorter times, i.e. those preceding the asymptotic self-similar regime (see also discussion in §4). These considerations allow one to classify the solution of the form (16) as a self-similar solution of the second kind (Zel'dovich & Raizer 1966).

The solutions developed here is based on the assumption that the solid block is undeformable. The behaviour of real granular materials differ from this model in the following: (i) the granules can be deformed, (ii) the pressure in the densely packed layer is non-uniform, since the pressure disturbances propagate from the shock front towards the piston not instantaneously, but with the finite speed of sound. To summarize the above, the solution developed here is valid when the absolute deformation of granules μ_s and speed of sound in the solid block a_s satisfy the following conditions:

$$\mu_s \ll \sigma(v_M - v_0)^{1/3}, \quad a_s \gg D_L^\infty / \rho_0.$$

For the majority of densely packed granular materials the velocity a_s is several hundreds of metres per second. This velocity is assumed to exceed significantly both the piston velocity (which for most vibrational machines is several metres per second) and the speed of the shock front propagation, given (20a), if ρ_0 is not very close to ρ_M . In this case and for sand-type (hard) materials the use of the undeformable solid block model is justifiable.

Note that both equations (20a, b) for the shock speed can be obtained from *purely mass and momentum conservation* considerations. Indeed choosing a control volume between $x = x_M$ and $x = x_F$, the steady-state (applicable to the asymptotic self-similar regime, where $x_F - x_M = \text{const.}$) mass and momentum conservation principles state that the rate of increase of the mass (momentum) within the dense layer is equal to the mass (momentum) flux across the shock front, i.e.

$$\begin{aligned} (D_L^\infty / \rho_0 - U) \rho_M &= D_L^\infty, \\ P_p^\infty + \rho_M (D_L^\infty / \rho_0 - U)^2 &= \rho_0 (D_L^\infty / \rho_0)^2, \end{aligned}$$

which immediately yields (20a, b). These considerations are not based on the existence of the fluidized domain behind the shock. They are valid for all non-conservative granular gases, including the case of absolutely inelastic collisions. In the latter case the extension of the fluidized domain tends to zero (see §3.2).

In the case of conservative gases, where no losses occur, another (purely self-similar) regime prevails, with the density $\rho = \rho_1$ behind the shock front. One can use the integral mass analyses, as above, with ρ_M replaced by ρ_1 , to obtain (22a) for the shock speed. This derivation also hinges upon energy considerations, which are embodied in the jump condition (8c), expressing continuity of the energy flux across the shock front.

Based on the above observations we can qualitatively discuss the effect of particle inelasticity on the extent of the fluidized domain. This domain is nil for absolutely inelastic collisions and tends to infinity for perfectly elastic collisions. The solution developed below concerns the intermediate situations, characterized by sufficiently small energy losses, for which the fluidized domain exists.

3.2. The high-density granular gas approximation

Let the initial mass density ν_0 be close to that of the most dense granular packing ν_M , so that

$$A_0 = 1 - \nu_0 / \nu_M \ll 1.$$

Then, using this condition, one can rewrite expressions (20a, b) for the long-time (stationary) values of the shock front speed and the granular pressure immediately behind the front:

$$D_L^\infty = U \frac{\rho_M}{\Delta_0}, \quad P_p^\infty = U^2 \frac{\rho_M}{\Delta_0}. \quad (23a, b)$$

Equations (19a), (19b) and (4) may be respectively rewritten in terms of the bulk velocity u , granular pressure P and kinetic energy E :

$$u(y) = U(1-y), \quad P(y) = P_p^\infty(1-y), \quad (24a, b)$$

$$\frac{E(y)}{m} = \frac{4y(1-y)}{3(1+e)\alpha_t} U^2, \quad y \equiv \Delta/\Delta_0, \quad (24c, d)$$

where $\Delta < \Delta_0 \ll 1$ and P_p^∞ is defined by (23b). Furthermore, use (23a), (24c) and (5) to reduce (21) to the following form:

$$a_1 \frac{d}{dz} [y(1-y)] + a_2(1-y) \frac{d}{dz} y = \frac{a_3}{\sigma \rho_M} y^{1/2} (1-y)^{3/2}, \quad (25)$$

where

$$a_1 = \frac{4}{3(1+e)\alpha_t}, \quad a_2 = 1 - C_2, \quad a_3 = \frac{\sqrt{3}C_0}{2\pi} \left[\frac{4}{(1+e)\alpha_t} \right]^{3/2}. \quad (26a-c)$$

The solution of (25) obeys the jump conditions (12c) at the shock wave front. Bearing in mind the definition (24d) of the variable y , one obtains the boundary condition for (25) in the form

$$y(0) = 1/\chi(e, \beta), \quad (27)$$

where $\chi(e, \beta)$ is given by (12d).

Solution of (25) may be written in the form

$$(2a_1 + a_2) \arcsin y^{1/2} - a_1 \left(\frac{y}{1-y} \right)^{1/2} = \frac{a_3 z}{\sigma \rho_M} + A, \quad (28)$$

where the constant A can be determined from the boundary condition (27).

The left-hand side of (28) may be approximated by a parabolic function, which together with boundary condition (27) enables (28) to be rewritten in the form

$$(a_1 + a_2) y^{1/2} = \frac{a_3 z}{2\sigma \rho_M} + \frac{a_1 + a_2}{\chi(e, \beta)}. \quad (29)$$

In the particular case of perfectly smooth particles i.e. $\alpha_t = 4/3$, $\beta = -1$ the accuracy of this approximation is better than a few percent. Now (29) may be reduced to the following form:

$$\Delta(z) = \Delta_0 \left[\frac{1}{\chi(e, \beta)} + \frac{a_3 z}{2\sigma \rho_M (a_1 + a_2)} \right]^2. \quad (30)$$

The maximal agitated mass Z_M behind the shock front, wherein collisional granular motion exists, may be evaluated from (30) and condition (18a), which may be rewritten as

$$\Delta(Z_M) = 0. \quad (31)$$

Solving (30) and (31) for Z_M , one obtains

$$Z_M = k_{z,d}(e, \beta) \sigma \rho_M, \quad (32)$$

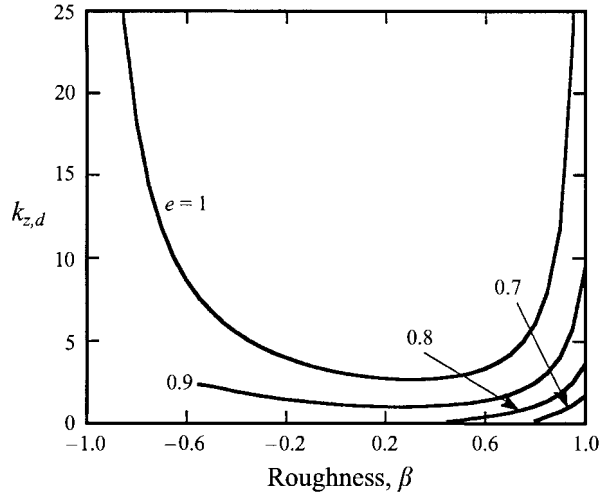


FIGURE 3. Dimensionless mass of the fluidized layer behind the shock front. High-density limit ($\nu_0 \sim \nu_M$).

where the coefficient $k_{z,d}(e, \beta)$ is given by the following explicit function of particle inelasticity and roughness:

$$k_{z,d}(e, \beta) = -2 \frac{\alpha_1 + \alpha_2}{\alpha_3 \chi(e, \beta)^{1/2}}. \quad (33)$$

As defined by (32) the coefficient $k_{z,d}$ has a clear physical meaning: it is equal to the number of rows in the random dense packing of the granular material.

Using (32), (33), one can rewrite (30) in the following form:

$$y = \frac{1}{\chi(e, \beta)} \left(\frac{Z_M - z}{Z_M} \right)^2. \quad (34)$$

Now we evaluate the average value of the energy of random motion E_{av} within the fluidized region which is generated by the steadily moving piston:

$$E_{av} = \frac{1}{Z_M} \int_0^{Z_M} E dz. \quad (35)$$

After substitution of E from (24c) jointly with (34) into the integral (35), one obtains

$$E_{av} = k_{E,d}(e, \beta) m U^2, \quad (36a)$$

where

$$k_{E,d}(e, \beta) = \frac{4[1 - 0.6/\chi(e, \beta)]}{9(1+e)\chi(e, \beta)\alpha_t}. \quad (36b)$$

Figures 3 and 4 present the dependence of the above dimensionless coefficients $k_{z,d}$, $k_{E,d}$ on the particles' collisional properties. One can see from figure 3 that $k_{z,d}$ tends to infinity for $e = 1$ and $\beta \rightarrow \pm 1$ (conservative gases), for which no dense layer is formed upon the piston. In these non-conservative cases the fluidized mass and energy increase indefinitely with time and are not described by (33), (36b). For intermediate values of β and $e = 1$, $k_{z,d}$ is finite owing to kinetic energy losses, which reach their maximum at about $\beta = 0.3$, where $k_{z,d}$ is minimal. Comparable curves corresponding to lower e have a similar character; however, they show lower values of $k_{z,d}$ owing to increasing

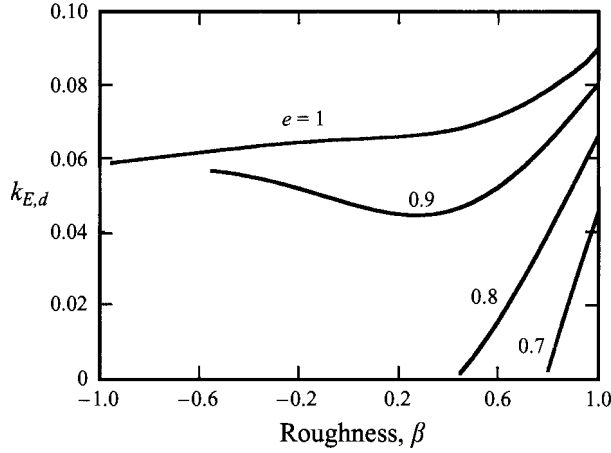


FIGURE 4. Dimensionless average kinetic energy in the fluidized layer behind the shock front. High-upstream-density limit ($\nu_0 \sim \nu_M$).

losses. The curve for $e = 0.9$ is bounded from the left by the maximal possible value of β for which the hydrodynamic equations (1) are valid (Goldshstein & Shapiro 1995). The curves plotted for lower values of e terminate at those values of β for which $k_{z,a}$ effectively vanishes. These cases correspond to large energy losses, for which the extension of the fluidized layers is less than one particle layer and the dense layer is formed immediately after the shock front. This may be seen directly from the Rankine–Hugoniot condition (8c); indeed for large losses (e.g. $e < 0.8$) the constants C_1 , C_2 appearing in (8c) approach unity, which implies that $g(\nu) \rightarrow \infty$, and, hence, $\nu = \nu_M$.

Figure 4 shows that for low values of the restitution coefficient (e.g. $e = 0.7$) $k_{E,d}$ decreases with β decreasing from 1, which is also explained by increasing kinetic energy losses. A similar curve plotted for $e = 0.9$ exhibits a minimum at $\beta \sim 0.3$, which corresponds to the maximal losses. However, the uppermost curve for $e = 1$ has a different β dependence, i.e. does not exhibit a minimum of $k_{E,d}$. This is explained by the rapid increase of $k_{z,a}$, and hence Z_M (occurring when $\beta \rightarrow -1$), which serves as a normalized value in the definition of $k_{E,d}$ (see (35)). Explicitly, both the integral in (35) and Z_M tend to infinity when $e = 1$ and $\beta \rightarrow \pm 1$; however their ratio remains finite. The limiting values of $k_{E,d}$ shown in figure 4 for $e = 1$ and $\beta = \pm 1$ do not reproduce the true value of $k_{E,d}$ for conservative gases, which may be shown to be 0.5 and depends neither on the initial density, nor the molecular nature of the gas.

3.3. Solution for arbitrary initial density

Integrate both sides of (21) from ν to ν_M , to obtain

$$Z(\nu_M) - Z(\nu) = \frac{2m}{\sigma^2 C_0} \left[\int_{\nu}^{\nu_M} F_E(\nu) dG_E(\nu) + \int_{\nu}^{\nu_M} F_\nu(\nu) dG_\nu(\nu) \right], \quad (37)$$

where

$$F_E(\nu) = \frac{UD_L^\infty}{ng(\nu)E(\nu)}, \quad G_E(\nu) = \left(\frac{E(\nu)}{mU^2} \right)^{1/2}, \quad G_\nu(\nu) = \left(\frac{\nu_0 - \nu_0}{\nu - \nu_M} \right)^{1/2}, \quad (38a-c)$$

$$F_\nu(\nu) = \frac{nE(\nu)(C_2 - C_1)\alpha_t/2 + (1 - C_2)P(\nu)}{ng(\nu)E(\nu)\rho_p} \left[\left(\frac{1}{\nu} - \frac{1}{\nu_M} \right) \frac{m(D_L^\infty)^2}{E(\nu)\nu_0} \right]^{1/2}, \quad (38d)$$

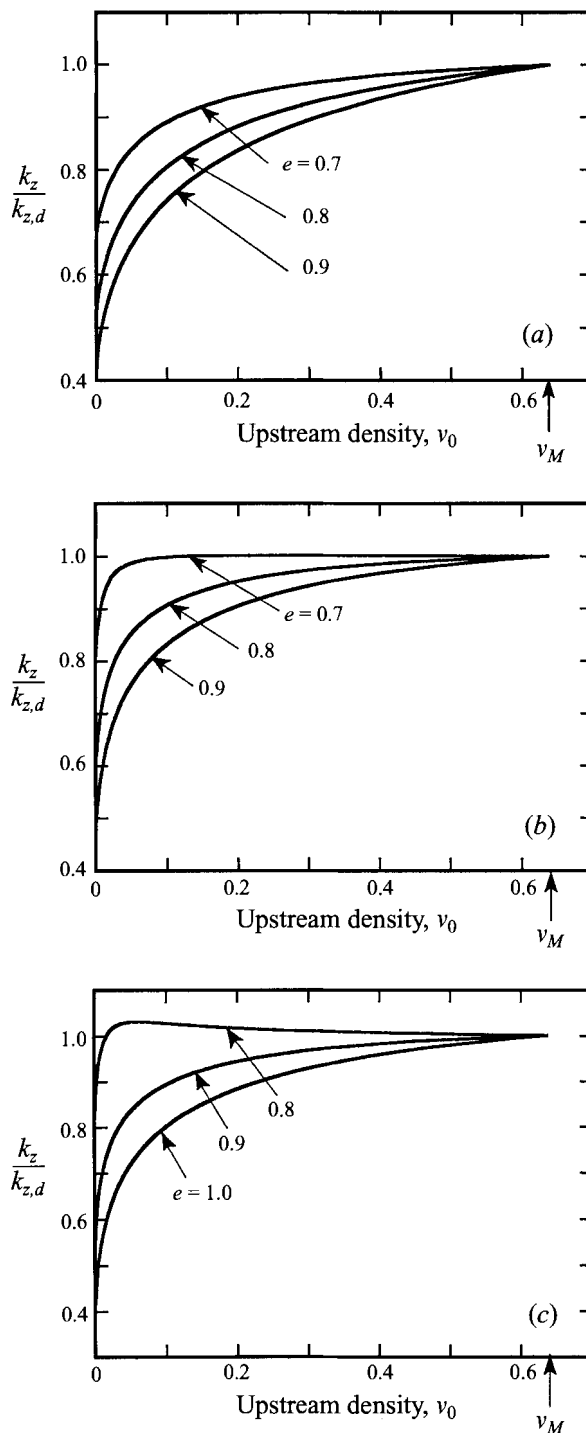


FIGURE 5. Normalized dimensionless mass of the fluidized layer behind the shock front $vs.$ upstream density: (a) $\beta = -1$, (b) $\beta = 1$, (c) $\beta = 0.8$.

which are of order unity for all $\nu_1 < \nu < \nu_M$. Similarly to the particular case of the high-density model (cf. (32)) we introduce here the amount of fluidized material $Z_M(\nu_M)$:

$$Z_M = \sigma \rho_M k_z(e, \beta, \nu_0, \nu_M), \quad (39)$$

for any arbitrary initial density, wherein

$$k_z(e, \beta, \nu_0, \nu_M) = \frac{\pi}{3\nu_M C_0} \left[\int_{\nu_1}^{\nu_M} F_E(\nu) dG_E(\nu) + \int_{\nu_1}^{\nu_M} F_\nu(\nu) dG_\nu(\nu) \right]. \quad (40)$$

This expression, with ν_1 related to ν_0 via (8c), was numerically integrated. The results are presented in figure 5(a-c) as the ratio of k_z to its high-density limiting value $k_{z,a}$ given by (33). One can see that the general effect of decreasing density ν_0 is to diminish k_z with respect to $k_{z,a}$. This can be explained by noting that with decreasing ν_0 the pressure P_p^∞ on the dense layer's edge behind the front also decreases, which results in a smaller fluidized mass.

The effect of the particle restitution coefficient upon $k_z/k_{z,a}$ is determined by the rate of change of each of the latter values with decreasing e . Clearly, $k_{z,a}$ decreases with decreasing e more rapidly than k_z , since for dense systems particle collisions (causing the losses) occur more frequently than in systems characterized by lower ν_0 . Alternatively, the fluidized mass of a more dissipative (characterized by a lower e) system exhibits a weaker dependence on ν_0 , than its higher- e counterpart. In particular, for $e = 0.7$ and $\beta = 1$, $k_z/k_{z,a} \sim 1$ down to almost $\nu_0 = 0.05$ (see figure 5b). Systems of smooth particles ($\beta = -1$) have a stronger ν_0 -dependence since their kinetic energy is distributed only between translational degrees of freedom, which promotes higher energy losses per collision.

The limiting case of elastic particles cannot be analysed for $|\beta| = 1$; however, it is shown in figure 5(c) for $\beta = 0.8$. The $k_z/k_{z,a}$ -curves for this case follow the same general trend, i.e. they are weakly affected by ν_0 (the most significant change for $e = 1$ amounts to a factor of 3.5).

Note that in most practical cases ($e < 0.9$ and intermediate β) not more than five particle layers can be fluidized. This theoretical result accords with experimental observations of vibrofluidized granular materials. Bachmann (1940) found that vibrated beds of large lead and glass spheres act as a single block when the initial depth of the bed exceeds six particle monolayers. In our recent contribution (Goldshtein *et al.* 1995) we found a gas-like behaviour of vibrated beds with about 20 monolayers. Hence, the solution of the problem of a steadily pushing piston allows us to predict the existence of the upper limit for the bed depth which may be fluidized, and estimate its value. However, in the case of vibrational agitation this upper limit depends also upon the vibrational parameters.

The effect of gas upstream density ν_0 on mass distribution within the fluidized layer is more dramatic when presented in physical coordinates. These data are given in figure 6, which shows the dependence of the density ν upon the dimensionless distance

$$\xi = \frac{x_M - x}{\sigma}, \quad (41a)$$

measured from the shock front (see figure 1). The length of the fluidized region may be obtained from (37) and the x, h relation, and may be expressed by

$$\xi_M(e, \beta, \nu_0, \nu_M) = \frac{\pi}{3\nu_M C_0} \left[\int_{\nu_1}^{\nu_M} \frac{F_E(\nu)}{\nu} dG_E(\nu) + \int_{\nu_1}^{\nu_M} \frac{F_\nu(\nu)}{\nu} dG_\nu(\nu) \right]. \quad (41b)$$

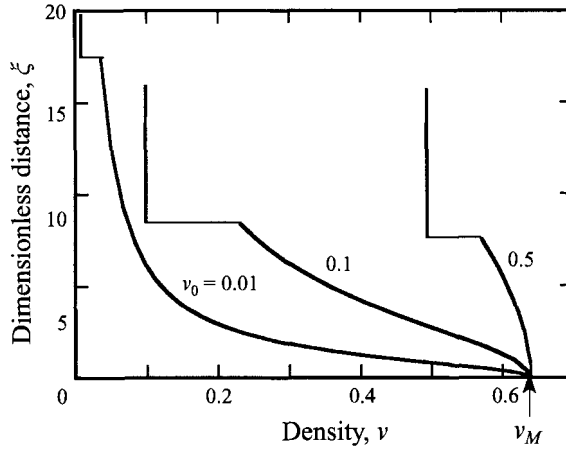


FIGURE 6. Density distribution along the length of the fluidized layer, $\beta = -1$, $e = 0.9$. ξ is measured from the edge of the dense layer towards the shock front.

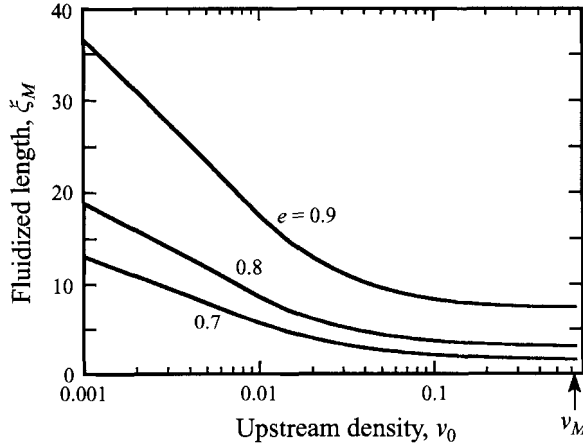


FIGURE 7. Dimensionless length of the fluidized layer behind the shock front vs. upstream density, $\beta = -1$.

One can observe in figure 6 jumps from $\nu = \nu_0$ to the value ν_1 determined by the condition (8b), followed by a monotonic increase of ν up to ν_M .

The dimensionless length ξ_M of the fluidized region is seen to increase with decreasing ν_0 (which is in contrast to Z_M , exhibiting the opposite behaviour, see figures 4 and 5a). This length is shown in figure 7 vs. ν_0 , for several e , where one can see that ξ_M is almost independent of ν_0 down to $\nu_0 = 0.1$. The extent of the fluidized region is, however, diminished with decreasing restitution coefficient, as a result of kinetic energy losses.

4. Discussion

We now estimate the time t_s required to attain the closest granular packing density at the piston surface. This may serve as a lower estimate of the time t_s required for achieving the asymptotic self-similar regime, for which the solution (16) is valid. It is

obvious that the density ρ_M at the piston is achieved during the time required for the shock wave to travel the mass distance Z_M . Expressing Z_M by

$$Z_M = \int_0^{t_s} D_L(t) dt,$$

and bearing in mind that D_L does not change significantly (see figure 2), one obtains

$$t_s \approx Z_M / D_L^\infty. \quad (42a)$$

Equations (20a), (42a) combined with the above result yield the following estimate:

$$t_s \approx \frac{\sigma}{U} k_z(e, \beta, \rho_0, \rho_M) \left(\frac{\rho_M}{\rho_0} - 1 \right). \quad (42b)$$

The coefficient k_z depends strongly on the inelasticity e , while the factor $(\rho_M/\rho_0 - 1)$ varies strongly with the upstream density ν_0 . In the case of large ν_0 and strong inelastic collisions one has $t_s \sim \sigma/U$. In this case relation (42b) predicts the attainment of closest packing density after the piston travels a distance of the order of one particle diameter. This means that $\xi_M \rightarrow 0$ as $e \rightarrow 0$. In this case the granular motion is, of course, non-hydrodynamic.

As follows from our analysis for $t \gg t_s$ the disturbed region may be subdivided into the densely packed solid block $Ut < x < x_M$ and the fluidized region $x_M < x < x_F$. According to (16d) and (20a) at these times the mass h_M of the solid block increases with t as

$$h_M = D_L^\infty t = \frac{U\rho_0 t}{1 - \rho_0/\rho_M}. \quad (43)$$

The corresponding physical length $x_M - Ut$ of the solid block may be obtained from (43) by division of h_M by ρ_0 . The dimensionless mass k_z and length ξ_M of the fluidized region given by (40), (41b) are independent of time t and of the piston speed U , and depend only on particle collisional properties and the upstream volume concentration.

We now comment on the applicability of the hydrodynamic equations for the description of granular flows of inelastically colliding particles. In Part 1 (Goldshtein & Shapiro 1995) necessary conditions for the existence of a hydrodynamic solution for the Boltzmann equation written for the granular gas have been formulated in terms of particle inelasticity and roughness. Sufficient conditions for the existence of such a solution should be determined for each specific problem. In this work we determined that the latter conditions are independent of piston velocity U but, rather, depend on the particle upstream density ν_0 . This is in contrast to shear-induced granular flows, where the existence of the collisional motion (described by the hydrodynamic solution) imposes constraints on the dimensionless velocity shear and the inelasticity $1 - e$, restricting both of them to small values (Jenkins & Richman 1985a). The existence and significance of the hydrodynamic solution of the present problem depends on the length of the fluidized region compared with the mean free path of the colliding granules and/or their size. In this respect we will note that the vibrofluidized behaviour of beds composed of about 5–10 granular monolayers is satisfactorily described by the hydrodynamic equations (Goldshtein *et al.* 1995).

The data on k_z, k_E obtained here may be used to interpret the results on shock wave propagation in vibrated granular layers (Goldshtein *et al.* 1995). This process occurs periodically, beginning from the moment when the freely falling layer meets the piston.

The average mass speed of wave propagation and pressure behind the shock was shown to be

$$D_L = \frac{2A\omega}{\Delta_0} \rho_M, \quad P_0 = \frac{4A^2\omega^2}{\Delta_0} \rho_M, \quad (44)$$

where A and ω are the vibrational amplitude and frequency, respectively, and $\Delta_0 = 1 - \nu_0/\nu_M \ll 1$. Bearing in mind that at the moment of contact the piston–layer relative velocity was shown to be close to $2A\omega$, one can clearly observe that the above formulae upon the substitution $U = 2A\omega$ reproduce equations (22a, b), here obtained by a rigorous treatment.

Goldshtein *et al.* (1995) derived the following expression for the average energy of the vibrated layer:

$$E_{av} = \frac{k(H)}{4} mA^2\omega^2, \quad (45)$$

which implicitly depends on the layer thickness h_m via a dimensionless coefficient $k(H)$ and the kinetic energy loss parameter

$$H = \left(\frac{\pi}{3}\right)^{1/2} \frac{(1-e^2)h_m}{\sigma}. \quad (46)$$

Using the relative layer–piston velocity $U = 2A\omega$, expression (45) may be rewritten in the form

$$E_{av} = \frac{k(H)}{16} mU^2, \quad (47)$$

which may be compared with expression (36a) for the average energy of the fluidized layer.

For layers composed of inelastic ($e = 0.88$), smooth ($\beta = -1$) particles and the vibrational regimes investigated by Goldshtein *et al.* (1995), coefficient $k(H)$ was measured and found to be in the range $0.122 < k(H) < 0.47$ or $0.01 \lesssim k(H)/16 \lesssim 0.03$. For the above values of collisional parameters the present calculations yield $k_{E,a} = 0.055$.

One can see, therefore, that the present self-similar solution predicts the average kinetic energy to be the same order of magnitude as the comparable quantity measured in vibrofluidized layers. Both of these values are considerably less than $k_{E,a}$ for conservative media (0.5). The differences between the calculated $k_{E,a}$ and measured $k(H)/16$ may clearly be attributed to the difference in shock wave propagation conditions. In the present problem the piston moves with constant velocity, sustaining the wave propagation regime. On the other hand, the vibrofluidized regime is sustained in a discontinuous manner, during piston–layer contact times which are very short compared with the vibrational period. During the rest of the period the kinetic energy induced by the shock wake wave dies out, which may explain lower values of $k(H)/16$, compared with $k_{E,a}$.

Another possible reason for the discrepancy is the difference in the thicknesses of the layers, which is infinite in the present model and finite ($h_m = 10$ – 20 particle monolayers) in the experiments of Goldshtein *et al.* (1995). In our treatment the latter parameter may, however, be identified as the length k_z of the fluidized region, given by (40). Using the value $k_z \sim 7\sigma$ calculated for $e = 0.9$, one can calculate from (44), (45), $k(H) = k(1.35) = 0.91$. Although no experimental data have been collected for such a small H , the above value of $k(H)$ may be compared with the value $k(H) = 0.80$ of this

coefficient calculated from the simplified model of the vibrated layers Goldshtein *et al.* (1995). One can see that in spite of apparent differences between the basic problem formulation treated here and the approximate model of the vibrofluidized bed, the two treatments yield close results for the average granular kinetic energy.

This research was in part supported by the Israel Science Foundation, administered by the Israel Academy of Sciences and Humanities and the Technion VPR Fund – Promotion of Sponsored Research – PBC. A. G. expresses his gratitude to Professor M. A. Goldshtik for encouragement and fruitful discussions on the subject of this paper.

Appendix

The dependence of α_t, α_r upon the inelasticity e and roughness β coefficients and the dimensionless rotary moment of inertia k were evaluated by Goldshtein & Shapiro (1995) as

$$\alpha_t = \frac{2}{3} \left(1 + \frac{a}{b + (a^2 + b^2)^{1/2}} \right), \quad \alpha_r = \frac{2}{3} \left(1 - \frac{a}{b + (a^2 + b^2)^{1/2}} \right), \quad (\text{A } 1 a, b)$$

where

$$a = (1 - \beta^2) \frac{1 - k}{1 + k} - 1 + e^2, \quad b = 2k \left(\frac{1 - \beta^2}{1 + k} \right). \quad (\text{A } 2 a, b)$$

In the above formulas $0 < e \leq 1$, $-1 \leq \beta \leq 1$ and $k = 0.4$ (the case of uniform spheres, considered here). We also impose the following restriction:

$$e \leq \left(\frac{2k}{1+k} - \beta \frac{1-k}{1+k} \right)^{1/2}, \quad (\text{A } 3)$$

which ensures monotonic dependences of the parameters α_t, α_r on the coefficients β, e (Goldshtein & Shapiro 1995).

Under condition (A 3) the coefficients C_0, C_1, C_2 appearing in the sink term are the following explicit and implicit functions of β, e :

$$C_0 = - \left(\frac{\pi}{2} \right)^{1/2} a_t^{3/2} \left[1 - e^2 + \left(\frac{1 - \beta^2}{1 + k} \right) \left(k + \frac{\alpha_r}{\alpha_t} \right) \right], \quad (\text{A } 4)$$

$$C_1 = \lambda \chi_k / \chi, \quad (\text{A } 5)$$

$$C_2 = \lambda \chi_c / \chi + N(F), \quad (\text{A } 6)$$

with

$$\lambda = - \left(\frac{\pi \alpha_t}{2} \right)^{1/2} \left[3(1 - e^2) + \left(\frac{1 - \beta^2}{1 + k} \right) \left(3k - 2 + \frac{\alpha_r}{\alpha_t} \right) \right], \quad (\text{A } 7)$$

$$\chi = \left(\frac{\pi \alpha_t}{2} \right)^{1/2} \left\{ \frac{3}{4} (1 - e^2) \alpha_t (3\alpha_t - \alpha_r) + \left(\frac{1 - \beta^2}{1 + k} \right) \frac{3}{4} [(3k - 3) \alpha_t \alpha_r + \alpha_r^2 - k \alpha_t^2] \right. \\ \left. + 4 \frac{\eta_2}{k} \left[3\eta_2 \alpha_t + \left(1 - \frac{\eta_2}{k} \right) (2\alpha_t - \alpha_r) \right] \right\}, \quad (\text{A } 8)$$

$$\chi_c = - \frac{3}{4} \alpha_t \alpha_r [1 - N(F)] + \frac{4\eta_2 \alpha_t}{(1 + e)k} \left[\eta_2 + \left(\frac{\eta_2}{k} - 1 \right) \frac{\alpha_r}{\alpha_t} \right], \quad \chi_k = - \frac{3}{4} \alpha_t \alpha_r, \quad (\text{A } 9 a, b)$$

$$N(F) = \frac{3}{2} (1 - e) + \left(\frac{1 - \beta^2}{1 + k} \right) \left(\frac{k + \alpha_r / \alpha_t}{1 + e} \right), \quad (\text{A } 10)$$

where
$$\eta_1 = \frac{1+e}{2}, \quad \eta_2 = \left(\frac{1+\beta}{1+k}\right)\frac{k}{2}. \quad (\text{A } 11 \text{ a, b})$$

In the particular case of perfectly smooth particles, i.e.

$$\alpha_t = \frac{4}{3}, \quad \alpha_r = 0, \quad \beta = -1, \quad (\text{A } 12 \text{ a-c})$$

(A 4)–(A 6) reduce to

$$C_0 = -\left(\frac{\pi}{2}\right)^{1/2} \alpha_t^{3/2}(1-e^2), \quad C_1 = 0, \quad C_2 = \frac{3}{2}(1-e). \quad (\text{A } 13 \text{ a-c})$$

REFERENCES

- ALDER, B. J. & HOOVER, W. G. 1968 Numerical statistical mechanics. In: *Physics of Simple Liquids*, pp. 79–114. North-Holland.
- ALDER, B. J. & WAINWRIGHT, T. E. 1960 Studies in molecular dynamics. II. Behavior of a small number of elastic spheres. *J. Chem. Phys.* **33**, 1439–1451.
- BACHMANN, D. 1940 Bewegungsvorgänge in schwingmühlen mit trockner mahlkörperfüllung. *Verfahrenstechnik Z. VDI-Beiheft* **2**, 43–55.
- CAMPBELL, C. S. 1990 Rapid granular flows. *Ann. Rev. Fluid Mech.* **22**, 57–92.
- CARNAHAN, N. F. & STARLING, K. E. 1969 Equations of state of nonattracting rigid spheres. *J. Chem. Phys.* **51**, 635–636.
- CHAPMAN, S. & COWLING, T. G. 1970 *The Mathematical Theory of Non-Uniform Gases*. 3rd edn. Cambridge University Press.
- CONDIFF, D. W., LU, W. K. & DAHLER, J. S. 1965 Transport properties of polyatomic fluids, a dilute gas of perfectly rough spheres. *J. Chem. Phys.* **42**, 3445–3475.
- COURANT, R. & FRIEDRICHS, K. O. 1948 *Supersonic Flow and Shock Waves*. Interscience.
- GOLDSHTEIN, A. & SHAPIRO, M. 1995 Mechanics of collisional motion of granular materials. Part 1. General hydrodynamic equations. *J. Fluid Mech.* **282**, 75–114.
- GOLDSHTEIN, A., SHAPIRO, M. & GUTFINGER, C. 1996 Mechanics of collisional motion of granular materials. Part 4. Expansion wave. *J. Fluid Mech.* (submitted).
- GOLDSHTEIN, A., SHAPIRO, M., MOLDAVSKY, L. & FICHMAN, M. 1995 Mechanics of collisional motion of granular materials: Part 2. Wave propagation through a granular layer. *J. Fluid Mech.* **287**, 349–382.
- GOLDSMITH, W. 1960 *Impact: The Theory and Physical Behavior of Colliding Solids*. E. Arnold.
- GRAD, H. 1949 On the kinetic theory of rarefied gas. *Commun. Pure. Appl. Maths* **2**, 331–407.
- HOMSY, G. M., JACKSON, R. & GRACE, J. R. 1992 Report of a symposium on mechanics of fluidized beds. *J. Fluid Mech.* **236**, 447–495.
- JENKINS, J. T. & RICHMAN, M. W. 1985a Grad's 13-moment system for a dense gas of inelastic spheres. *Arch. Rat. Mech. Anal.* **87**, 355–377.
- JENKINS, J. T. & RICHMAN, M. W. 1985a Kinetic theory for plane flows of a dense gas of identical, rough, inelastic, circular disks. *Phys. Fluids* **28**, 3485–3494.
- JENKINS, J. T. & SAVAGE, S. B. 1983 A theory for rapid flow of identical, smooth, nearly elastic, spherical particles. *J. Fluid Mech.* **130**, 187–202.
- LAN, Y. & ROSATO, A. D. 1995 Macroscopic behavior of vibrating beds of smooth inelastic spheres. *Phys. Fluids* **7**, 1818–1831.
- LUDING, S., HERRMANN, H. J. & BLUMEN, A. 1994 Simulations of two-dimensional arrays of beads under external vibrations: Scaling behavior. *Phys. Rev. E* **50**, 3100–3108.
- LUN, C. K. K. 1991 Kinetic theory for granular flow of dense, slightly inelastic, slightly rough spheres. *J. Fluid Mech.* **233**, 539–559.
- LUN, C. K. K. & BENT, A. A. 1994 Numerical simulations of inelastic frictional spheres in simple shear flow. *J. Fluid Mech.* **258**, 335–353.
- LUN, C. K. K. & SAVAGE, S. B. 1986 The effect of an impact dependent coefficient of restitution on stresses developed by sheared granular materials. *Acta Mech.* **63**, 15–44.

- LUN, C. K. K. & SAVAGE, S. B. 1987 A simple kinetic theory for granular flow of rough, inelastic, spherical particles. *Trans. ASME E: J. Appl. Mech.* **54**, 47–53.
- LUN, C. K. K., SAVAGE, S. B., JEFFERY, D. J. & CHEPURNIY, N. 1984 Kinetic theories for granular flow: inelastic particles in Couette flow and slightly inelastic particles in a general flow field. *J. Fluid Mech.* **140**, 223–256.
- MATVEEV, S. K. 1983 Rigid-particle gas model with allowance for inelastic collisions. *Izv. Akad. Nauk SSSR Mekh. Zhidk. Gaza* **6**, 12–16.
- MCCOY, B. J., SANDLER, S. I. & DAHLER, J. S. 1966 Transport properties of polyatomic fluids. IV. The kinetic theory of a dense gas of perfectly rough spheres. *J. Chem. Phys.* **45**, 3485–3500.
- OGAWA, S., UMEMURA, A. & OSHIMA, N. 1980 On the equations of fully fluidized granular materials. *Z. Angew. Math. Phys.* **31**, 483–493.
- RASKIN, KH. I. 1975 Application of the methods of physical kinetics to problems of vibrated granular media. *Dokl. Acad. Nauk SSSR* **220**, 54–57.
- SAVAGE, S. B. 1988 Streaming motions in a bed of vibrationally fluidized dry granular material. *J. Fluid Mech.* **194**, 457–478.
- THEODOSOPULU, M. & DAHLER, J. S. 1974 The kinetic theory of polyatomic liquids. II. The rough sphere, rigid ellipsoid, and square-well ellipsoid models. *J. Chem. Phys.* **60**, 4048–4057.
- ZEL'DOVICH, YA. B. & RAIZER, YU. P. 1966 *Physics of shock waves and high temperature hydrodynamic phenomena*. Academic.